Earth and Planetary Science Letters 271 (2008) 233–240

Contents lists available at ScienceDirect

Earth and Planetary Science Letters

journal homepage: www.elsevier.com/locate/epsl

Trench migration, net rotation and slab–mantle coupling

F. Funiciello [a,*], C. Faccenna [a], A. Heuret [a,b], S. Lallemand [b], E. Di Giuseppe [a,c], T.W. Becker [d]

[a] Dip. Scienze Geologiche, Università degli Studi « Roma TRE », Largo S. Leonardo Murialdo 1, 00146 Roma, Italy
[b] Laboratoire Géosciences Montpellier, Université Montpellier 2, CNRS, CC. 60, place E. Bataillon, 34095 Montpellier cedex 5, France
[c] Institute of Geophysics, ETH-Honggerberg 8093-CH Zurich Switzerland
[d] Department of Earth Sciences, University of Southern California Los Angeles, USA

ARTICLE INFO

Article history:
Received 31 May 2007
Received in revised form 28 March 2008
Accepted 8 April 2008
Available online 20 April 2008

Editor: C.P. Jaupart

Keywords:
lithosphere/mantle viscosity
laboratory models
subduction
trench velocity
plate velocity
net rotation

ABSTRACT

Laboratory models have been conducted to improve our understanding of the role that the resistance of the slab to bending and its coupling to the ambient mantle play in subduction dynamics over geological time scales. Our models are set up with a viscous plate of silicone (lithosphere) subducting under negative buoyancy in a viscous layer of glucose syrup (mantle). For our study, the lithosphere/upper mantle viscosity contrast has been systematically varied, from ~10 to ~10^5 in order to explore the parameter space between weak and strong slab dynamics. We found that subduction is characterized by a retreating mode for viscosity ratios >10^4, by the coexistence of a retreating mode and an advancing mode for viscosity ratios between ~10^4 and ~10^2, and quasi-stationary, Rayleigh–Taylor like behaviour for ratios <10^2. By combining our experimental results and kinematic data from current subduction zones in four reference frames which differ in the amount of net rotation, we infer that a lithosphere/upper mantle viscosity contrast of 150–500 is necessary to obtain realistic trench/subducting plate velocity ratios as well as the variability of subduction styles observed in nature.

1. Introduction

Experimental data and observations indicate that the old oceanic lithosphere is strong (Kohlstedt et al., 1995). During its journey from the ridge to the trench the cold temperature of the surface makes the oceanic lithosphere stiffer than the underlying mantle, allowing its near rigid motion. However, the evolution and effective strength of the lithosphere once bent at the trench and sinking into the mantle is still poorly understood. Generating plate-like behaviour requires the weakening of the plate margins (Bercovici, 1996; Moresi and Solomatov, 1998; Tackley, 1998; Trompert and Hansen, 1998), which may permanently reduce lithospheric strength during its descend into the deep mantle. The incomplete knowledge of the mechanical behaviour of the subducting lithosphere is reflected in choices for published subduction models, where viscosity ratios between the lithosphere and mantle range between unity and four orders of magnitude, or more (e.g. Kincaid and Olson, 1987; Davies, 1995; Griffiths et al., 1995; Guillou-Frottier et al., 1995; Zhong and Gurnis, 1995b; Ratcliff et al., 1997; Solomatov and Moresi, 1997; Funiciello et al., 2003). The goal of this work is to contribute to defining the slab resistance and its coupling with the ambient mantle. So far, approaches quantifying both absolute and relative values of the lithosphere and mantle viscosity have included observations from post-glacial isostatic adjustment (Mitrovica and Peltier, 1991; Mitrovica and Forte, 1997), modeling the geoid and dynamic topography using density anomaly distributions coming from seismic tomography (e.g. Ricard et al., 1989; King and Masters, 1992), study of the high-temperature and high-pressure deformation properties of mantle rocks in the laboratory (e.g. Ashby and Verall, 1978; Karato, 1997), study of small variations in the Earth's rotation (e.g. Sabadini and Peltier, 1981), and modelling of plate kinematics (e.g. Lithgow-Bertelloni and Richards, 1998; Doglioni et al., 2006; Crespi et al., 2007). In particular, these studies attributed to the upper mantle viscosity and lithosphere/upper mantle viscosity ratio values, ranging from 10^{19} to 10^{21} Pa s and 10^1 to 10^3, respectively. Here, we propose an alternative way to constrain the ratio of lithospheric to mantle, η_l / η_{um}, viscosity. Our objective is to use the rate of trench migration as a proxy of the resistance exerted by the mantle to the lateral migration of the slab.

Lithosphere sinks into the mantle, attaining a lateral migration (Spence, 1977; Carlson and Melia, 1984; Garfunkel et al., 1986). For a given slab dip, the horizontal component of the subduction velocity can be directly estimated by the facewise translation (in a direction normal to the trench) of trenches over the Earth's surface. Lateral trench migration is accommodated by toroidal return flow around slab edges or slab windows (e.g. Buttles and Olson, 1998; Lithgow-Bertelloni and

* Corresponding author. Tel.: +39 06 57338058; fax: +39 06 57338201.
E-mail addresses: ffunicie@uniroma3.it (F. Funiciello), faccenna@uniroma3.it (C. Faccenna), harnauld@uniroma3.it (A. Heuret), lallemand@gm.univ-montp2.fr (S. Lallemand), erika.digiuseppe@tomo.ig.erdw.ethz.ch (E. Di Giuseppe), twb@usc.edu (T.W. Becker).

0012-821X/$ – see front matter © 2008 Elsevier B.V. All rights reserved.
doi:10.1016/j.epsl.2008.04.006

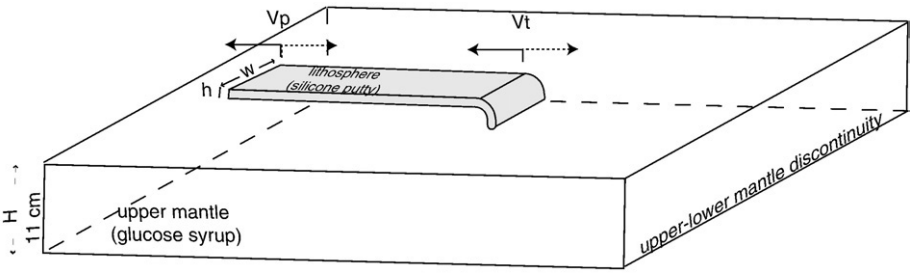

Fig. 1. Experimental setup. The lithosphere is simulated by a silicone plate of constant density (1490 kg cm^{-3}), viscosity (3.6×10^5 Pas), and length (40 cm) and variable width w and thickness h. The silicone plate floats in the middle of a large box to minimize possible boundary effects. The upper mantle is simulated by means of a range of glucose syrups, always 11 cm thick but with slightly variable densities ρ_m and strongly variable viscosities η_m. V_t and V_p are for trench velocity and plate velocity. Plain and dotted arrows refer to positive and negative velocities, respectively.

Richards, 1998; Kincaid and Griffiths, 2003; Funiciello et al., 2004; Funiciello et al., 2006; Piromallo et al., 2006). However, the dependence of trench velocity on mantle viscosity has not yet been tested.

Here, we conduct new and reanalyze old laboratory models to evaluate the dependency of trench migration on slab/mantle coupling. For this purpose, the lithosphere/upper mantle viscosity contrast has been systematically varied between ~10 and ~10^5. Assuming that trench migration of a simplified experimental slab can plausibly represent the natural behaviour of subducting lithosphere, we compared modelling results to present-day trench kinematics.

Firstly, we describe the set-up of our three dimensional (3-D), dynamically, self-consistent models and results. Secondly, we separately review observations of natural trench velocities in four different reference frames – hot spot reference frame and no net rotation (NNR) – which offer a wide range of net rotations between the lithosphere and deep mantle. Finally, we discuss modeling results and then tie those results back into the global plate tectonic picture. The comparison between the scaling rules deduced from the experimental data set and the statistical analysis of natural data gives constraints on the long term lithosphere/upper mantle viscosity contrast and, in turn, on the resistance of the slab.

2. Laboratory models

2.1. Experimental setting

Our laboratory models simulate subduction as a linearly viscous, two-layered system (Fig. 1). They are properly scaled to reproduce gravitational driving forces and viscous resistive forces active in natural settings (Weijermars and Schmeling, 1986; Faccenna et al., 1999; Funiciello et al., 2003) (see the Supplementary Material for a comprehensive treatment of the forces at work in the experimental system). The upper layer simulates a subducting oceanic lithosphere and is composed of highly-viscous and high viscosity and density silicone putty (Table 1). The lower layer set up a homogeneous upper mantle and is composed of low-viscous and low-dense glucose syrup (Table 1). The bottom of the box mimics the 660 km discontinuity.

Table 1
Parameters used in the selected experiments and in nature

PARAMETER			NATURE	MODELS
g	Gravitational acceleration	$m\times s^{-2}$	9.8	9.8
Thickness				
h_l	Oceanic lithosphere	m	$(60–100)\times10^3$	0.006–0.017
H	Upper mantle		6.6×10^5	0.11
Density				
ρ_l	Oceanic lithosphere	$kg\times m^{-3}$	3 300–3260	1 490
ρ_{um}	Upper mantle		3 220	1 415–1 460
Viscosity				
η_l	Oceanic lithosphere	$Pa\times s$	10^{22}–10^{24}	$3.6\cdot10^5$ (±5%)
η_{um}	Upper mantle		10^{19}–10^{21}	1–10^5(±20%)

We attempted to reduce the effect of boundary conditions as much as possible (Funiciello et al., 2004). The upper plate floats in the centre of a large Plexiglas tank ($80\times80\times20$ cm^3) filled with glucose syrup. We allowed a distance as large as possible between the plate and box sides (>20–30 cm). The plate subducts under negative buoyancy once its leading edge is manually pushed into the glucose syrup to a depth of 3 cm (corresponding to ≈180 km in nature), with an angle of ~30° (Funiciello et al., 2003). The plate is free at its trailing edge ("free ridge" sensu Kincaid and Olson, 1987), allowing a self-consistent response. Therefore, plates are completely surrounded by fault zones whose equivalent viscosities are the same as the upper mantle. These conditions guarantee the full mobility of the plate. This experimental setup implies the following assumptions and limitations that are detailed in Funiciello et al. (2003) and Bellahsen et al. (2005): 1) viscous rheology; 2) an isothermal system; 3) no external background flow, and 4) upper/lower mantle discontinuity as an impermeable barrier.

Experimental parameters are listed in Table 1. The scale factor for length is 1.6 10^{-7} (1 cm in the model corresponds to 60 km in nature), the scaling density factor between the oceanic subducting lithosphere and the upper mantle has been varied between 1.02 and 1.05, exploring the range of likely natural density contrasts (Cloos, 1993; Afonso et al., 2007). Further details on scaling can be found in Funiciello et al. (2006).

150 models have been performed by changing the subduction geometric (h, w; Fig. 1) and rheological (η_l/η_{um}, ρ_l/ρ_{um}) parameters. In particular, the lithosphere/upper mantle viscosity ratio (η_l/η_{um}) has been varied between ~10^1 and 10^5. The selected mantle viscosity field allows us to obtain laminar flow of the fluid in the limit of a small Reynolds number (10^{-1}–10^{-7}). Experiments have been performed at least twice to ensure reproducibility.

Each model is monitored using a sequence of digital pictures taken in lateral and top views. Afterwards, the trench (V_t) and subducting plate velocity (V_p) along the centreline, in the box reference frame, and the dip of the slab are measured during the steady-state phase reached after the slab-660 km discontinuity, using image-processing tools.

Plate velocity is defined as positive when directed toward the trench (Fig. 1). Subduction velocity, V_s, is determined to be the sum of the trench and plate velocities: $V_s = V_t + V_p$.

2.2. Modelling results

All the models show the typical sequence of three phases, as extensively described in Funiciello et al. (2003) and Bellahsen et al. (2005): (phase 1) progressive acceleration of the slab during its sinking into the mantle, (phase 2) transient slab/660 km discontinuity interaction, and (phase 3) steady state subduction with the slab lying on the 660 km discontinuity. The subduction during the steady-state phase can be characterized by an "advancing" or "retreating" trench style (Bellahsen et al., 2005). As a general rule, the advancing trench style is characterized by a steeper slab and fast plate motion, whereas

the retreating trench style is characterized by a shallow dip slab and slow plate velocity. In both styles, lateral trench migration allows considerable amounts of mantle to be displayed around the slab (Funiciello et al., 2004).

Fig. 2 summarizes the subduction geometry and kinematics (V_s) as a function of η_l / η_{um} observed for each model during the steady-state phase. V_s is normalized by a characteristic velocity, $V_{stokes}=\Delta\rho ghH / \eta_m$, obtained for a Stokes sinker using reference parameters for a standard subduction system (Table 1). Adopting a normalized V'_s, the dataset is homogenized for variations in $\Delta\rho$ and h occurring in the experimental dataset. Fig. 2 also includes data from the two Schellart' (2004) models characterized by similar boundary conditions (exp. n° 11, 12).

All the models follow a specific linear trend expressed by the function η_l / $\eta_{um}=(2.7\times10^5)\times V_s+1393$ ($R=0.9$). It is possible to distinguish three different fields:

1) η_l / $\eta_{um}>>10^4$. Subduction occurs with the highest V'_s and mainly shows the retreating mode behaviour, regardless of w, h and $\Delta\rho$ which are varied widely between 5 and 30 cm, 1.0 and 1.6 cm, and 40 and 100 kg cm^{-3}, respectively. The advancing mode can occur only for extremely thin plates. V'_s is partitioned between a very low V_p and a high V_t, which increases with increasing η_l / η_{um}. In particular, V_t spans between 80 and 99% of V'_s. Retreating slabs attain a forward bending shape, characterized by an average shallow dip of ~ 30° which increases with decreasing η_l / η_{um} reaching a maximum of. ~ 50°. The subducting lithosphere is never deformed and the trench maintains its straight shape during the entire subduction history, even for the widest plates.
2) η_l / $\eta_{um}=10^2$–10^4. Subduction can occur with either advancing or retreating modes depending on w, h and $\Delta\rho$. In our models, w has been varied between 5 and 30 cm, h between 0.6 and 1.7 cm and $\Delta\rho$ between 60 and 100 kg cm^{-3}. Narrow/thin/heavy plates favour the retreating mode, while wide/thick/less dense plates prefer to advance (see Bellahsen et al., 2005 for details on the specific contribution of these parameters).
   The retreating mode is characterized by trench retreat, shallowest dip (~65°), and low subducting plate motion rates. V_t always represents the dominant kinematic contribution being 60–99% of V'_s. On the contrary, in the advancing mode V_p enlarges its contribution, assuming a leading role (up to 60%) in controlling V'_s. Under this kinematic condition, the slab attains an overturned shape characterized by a steep dip (≥90°).
   The subducting lithosphere is deformed and the degree of deformation increases with decreasing η_l / η_{um}. The trench is always oceanward convex in both retreating and advancing modes of subduction. Confirming what was already expressed by Morra et al. (2006), the wider the plates, the strongest is the trench bending. Schellart's data (2004) fit this field. However, since Schellart's models did not explore a wide variability in lithospheric parameters, they showed only a retreating trench behavior.
3) η_l / $\eta_{um}<10^2$. The subduction process is quasi-stationary. Both trench and plate motion are very small and downwelling akin to a Rayleigh–Taylor instability develops rather than a typical subduction structure. The slab is strongly deformed both at the surface, where the trench becomes oceanward convex, and at depth.

3. Subduction zones trench kinematics

The final goal of our work is the definition of the slab resistance and its coupling with the ambient mantle over the geological time scale by using the rate of trench migration as a proxy of the resistance offered by the mantle to the slab motion. For this purpose, we explore global present-day trench kinematics to be compared with experimental data.

3.1. Are trenches advancing or retreating?

Despite that trench motion plays a primary role in defining tectonic regimes (Carlson and Melia, 1984; Faccenna et al., 2007), its contribution cannot be directly measured. Subtracting the permanent deformation – back-arc extension or shortening – from the overriding plate gives the arc sliver motion. This is akin to trench motion, but only if tectonic erosion or accretion processes at the trench are negligible (Lallemand, 1995). This approximation can indeed introduce a quite

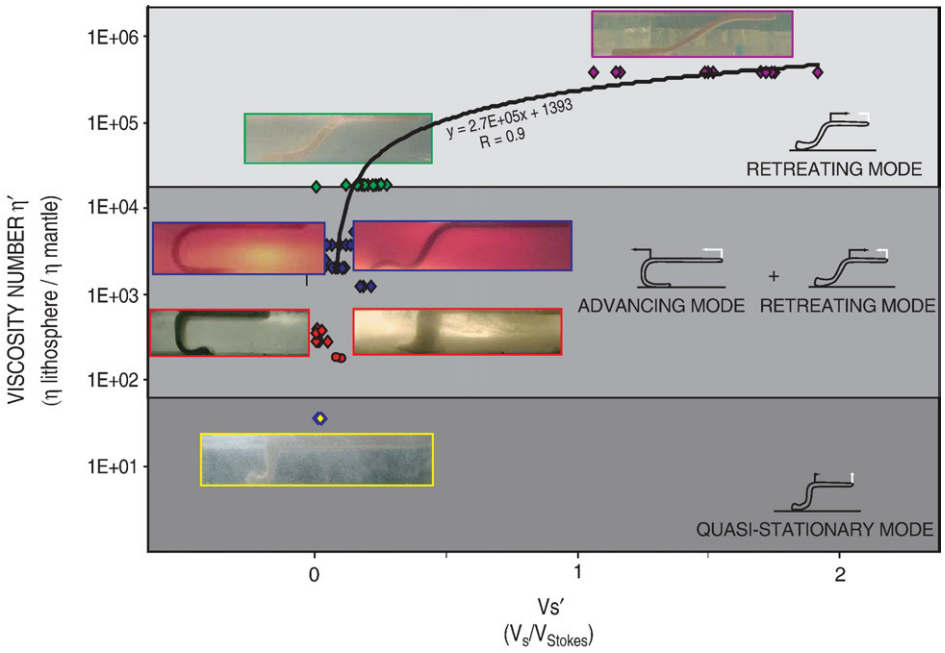

Fig. 2. Diagram showing the behaviour of free ridge (sensu Kincaid and Olson, 1987) laboratory models with different slab/mantle ratios η' and normalized subduction velocities (V_s divided by a normalized Stokes velocity to remove the effect of buoyancy changes for different mantle viscosities). Diamond colour refers to models having comparable behavior. Data from Schellart (2004) are represented by circles. For each identified group of models, a lateral view of the steady state stage of the evolution is shown. Grey areas are approximate divisions of model behavior. The black line identifies the linear regression existing between all points.

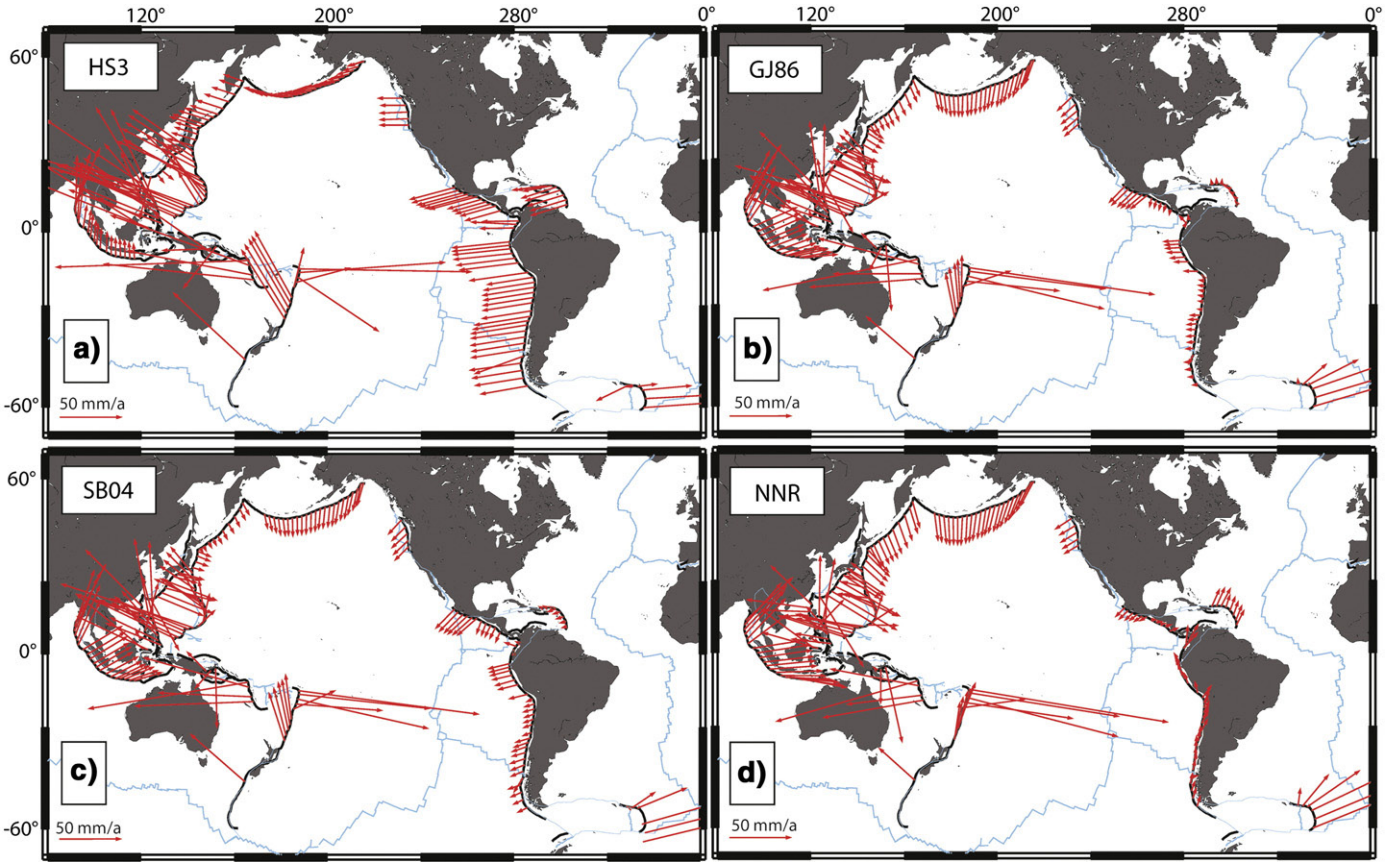

Fig. 3. Normal component of trench velocity $V_{t(n)}$ in four absolute reference frames: (a) hot spot reference frame of Gripp and Gordon (2002), which analyses the Pacific hot-spot track; (b) hot spot reference frame of Gordon and Jurdy (1986), which considers both the Indo-Atlantic and the Pacific hot-spot tracks; (c) hot spot reference frame of Steinberger et al. (2004), which investigates only the Indo-Pacific hot-spot tracks; (d) no-net-rotation reference frame (Gripp and Gordon, 2002). Reference velocity is indicated at the bottom-left of each panel.

large uncertainty into trench velocity estimates (see Doglioni, 2008 for discussion). Few analyses have focused on the velocity of natural trenches. First, Carlson and Melia (1984) analysed the pattern of trench migration of the Izu–Bonin–Marianas trench, showing that the Marianas trench is actually advancing in the hot-spot reference frame towards the Philippine Sea overriding plate. Garfunkel et al. (1986), on the other hand, also showed that according to the fixed deep hotspot model of Morgan (1982), over long geological term, Pacific trenches usually retreat backward towards the ocean. Jarrard (1986) gave the first exhaustive review of convergent margins kinematics pointing out that only a few trenches are advancing, whereas the majority are retreating. Recently, Sdrolias and Muller (2006) reconstructed the position of the Pacific trenches over the Tertiary using an updated dataset of paleoceanic age grids associated with a moving Atlantic–Indian Ocean hot spot reference frame (O'Neill et al., 2005), recognizing the dominant rollback motion of trenches.

These results are often in contrast for two main reasons. First, the rate of back-arc deformation is usually poorly known. Geodetic data are now available on most of the back-arc belts, but their short-term rates may differ from the long-term geological ones. Moreover, back-arc deformations are often not considered unless registered by back-arc spreading. For instance, Sdrolias and Muller (2006), reconstructed the position of the Andean trenches from the absolute motion of the Americas, but neglected the shortening absorbed by the Andes build up. Second, the velocity of plates is often described using different reference frames. Common reference frames use tracks of deep hot spots to unravel plate velocity, assuming hot spot fixity (Morgan, 1971). The discovery of relative mismatches between tracks since the Late Cretaceous (Raymond et al., 2000) allows the proposition of Indo-Atlantic and Pacific independent reference frames (Gordon and Jurdy, 1986; Steinberger, 2000; Gripp and Gordon, 2002; O'Neill et al., 2005). Alternative models adopt shallow hot spot (rooted in the astenosphere) reference frame substantially increasing plate velocity and net rotation (Doglioni et al., 2007). Finally, the no net rotation (NNR) reference frame is obtained assuming no net rotation of the lithosphere as a whole; i.e. the sum of the absolute motion of all plates weighted by their area is equal to zero.

Trench migration is sensitive to the adopted reference frame because its magnitude is comparable with the net rotation amplitude.

3.2. The kinematic database

We illustrate the kinematics of trenches using an updated database of worldwide subduction zones (Heuret, 2005; Heuret and Lallemand, 2005; Lallemand et al., 2005). The parameter selected for this study – – V_t – has been sampled at 220 km trench intervals along present-day oceanic subduction zones where slabs have already reached 660 km depth. The deformation of the back-arc region was taken from available geodetic data. The adopted approach suffers from comparison between different time-scales, but it has the advantage of including quantitative measures over most of the analysed regions. The normal component of trench motion, $V_{t(n)}$, has been plotted in four different reference frames (Fig. 3). In particular, we consider the hot spot references frame of *Gripp and Gordon* (2002; HS3; Fig. 3a), which analyzes the Pacific hot-spot track, *Gordon and Jurdy* (1986; GJ86; Fig. 3b) which considers both the Indo-Atlantic and the Pacific hot-spot tracks, Steinberger et al. (2004; SH04; Fig. 3c), which includes only the Indo-Pacific hot-spot tracks, and finally, the no-net-rotation reference frame (*Gripp and Gordon*, 2002; Fig. 3d; NNR). In all reference frames trenches both advance and retreat (Figs. 3–4, Table 2). Trench retreat predominates in GJ86, SH04 and NNR, representing 70%, 70% and 61%

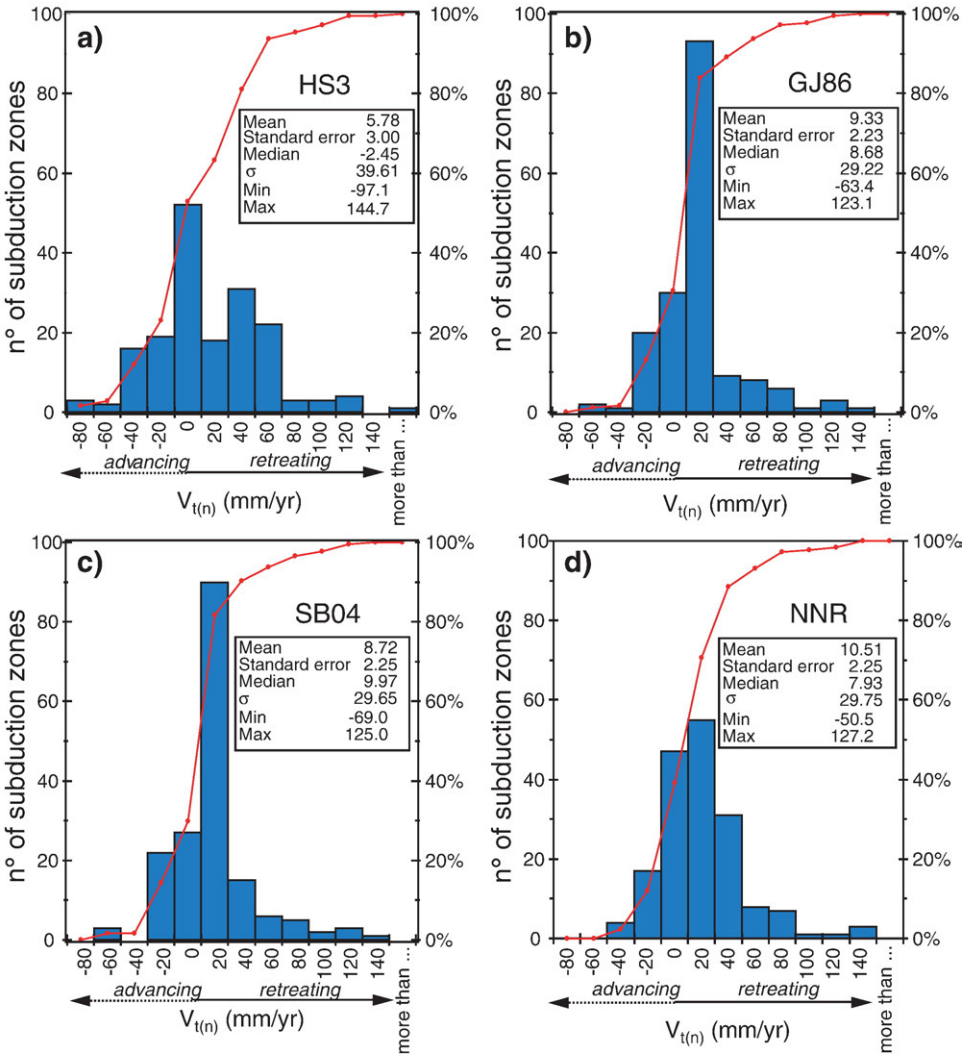

Fig. 4. Frequency plot of $V_{t(n)}$ for the 174 trench segments investigated in four absolute reference frames: (a) HS3; (b) GJ86; (c) SB04; (d) NNR. Each panel summarizes also the statistical analysis performed on the different datasets.

of all trench segments, respectively (Fig. 4, Table 2). On the contrary, trench motion is near equally partitioned between advance (53%) and retreat (47%) in HS3 (Fig. 4, Table 2). The mean trench velocity ($\Sigma V_{t(n)}/n$) is positive in all reference frames.

The four reference frames differ by the amount of net rotation of the lithosphere with respect to the mantle, which is maximum in HS3 with peak velocity 4.9 cm yr^{-1} and null by definition in NNR (Table 2). Being that $V_{t(n)}$ is only of the order of few cm yr^{-1} (Fig. 4), the change in the reference frame easily produces a switch of the trench migration from retreating to advancing. A striking example of how variation in net rotation can influence trench kinematics is evident in South America, where the trench is stationary in NNR, and slowly and rapidly retreating in GJ86/SH04 and HS3, respectively (Fig. 3). On the other side of the Pacific, the Kamchatka–Kuril–Japan trench is retreating for NNR, GJ86 and SH04, whereas it is advancing in HS3 (Fig. 3). Kermadec, Izu–Bonin–Marianas and Java-Sumatra conversely, are advancing, though at different rates, in all reference frames (Fig. 3). In general, the $V_{t(n)}$ variability decreases with a reduction of the net rotation (Fig. 4, Table 2). Hence, the maximum variability is observed in HS3, where the trench migration velocity varies from a minimum of −9.7 cm yr^{-1} (trench advance) to a maximum of 14.5 cm yr^{-1} (trench retreat) (Fig. 4, Table 2), whereas NNR shows the higher percentage of

Table 2
Main characteristics of the four reference frames adopted in this study

			HS3 *Gripp and Gordon (2002)*	GJ86 *Gordon and Jurdy (1986)*	SB04 *Steinberger et al. (2004)*	NNR - Nuvel1A *Gripp and Gordon (2002)*
hot spots			Pacific hot spots	Atlantic and Pacific hot spots	Indo-Atlantic hot spots	-
maximum rate of net rotation (cm yr^{-1})			4.9	1.3	1.8	0 (by definition)
trench motion	retreat	$\Sigma V_{t(n)}/n$ cm yr^{-1}	3.9	2.2	2.2	2.6
		$V_{t(n)max}$ cm yr^{-1}	14.5	12.3	12.5	12.7
		% subduction zone length	47%	70%	70%	61%
	advancing	$\Sigma V_{t(n)}/n$ cm yr^{-1}	2.4	2.0	2.2	1.4
		$V_{t(n)max}$ cm yr^{-1}	9.7	6.3	6.9	5.1
		% subduction zone length	53%	30%	30%	39%

not moving trenches (Fig. 4). We also observed that results for GJ86 and SH04 are considerably similar (Figs. 3–4, Table 2), as expected given their similar NR Euler poles.

4. Reconciling models to nature: insights into the slab–mantle coupling

Our models are designed to understand the role played by slab/mantle coupling in controlling subducting plate kinematics. The work is complementary to Bellahsen et al. (2005), where the role of several other parameters (plate thickness, plate density, plate width and plate thickness) have been already tested. We varied lithosphere/upper mantle viscosity contrast between ~10 and ~10^5. According to Bellahsen et al. (2005), we identified two styles of subduction, differentiated by the way the velocity of subduction is partitioned between trench and plate velocity during the steady-state phase: the "retreating mode" is characterized by a shallow, dipping, slowly moving subducting lithosphere while the trench rolls oceanward, whereas the "advancing mode" is characterized by a steeper slab and fast plate motion. In particular, we have identified that the retreating mode of subduction is developed for $\eta_l/\eta_{um} > 10^4$, subduction characterized by both a retreating and an advancing mode, distinguishes systems with η_l/η_{um} ranging between ~10^4 and ~10^2, while for $\eta_l/\eta_{um} < 10^2$, the subduction process is almost stationary (Fig. 2).

Giving our laboratory results, we assume that the rate and the style of trench migration can be used as a proxy of the resistance offered by the mantle to lateral slab migration, and moreover to estimate the natural lithosphere/upper mantle viscosity ratio.

Natural subduction zones show both advancing and retreating trenches. This characteristic is independent of the reference frame (Fig. 3, Table 2) which only moderately affects the overall data distribution (Fig. 4). We found that this bimodal trench behavior is experimentally observed only for η_l/η_{um} ranging between ~10^2 and 10^4 (Fig. 2). This viscosity range also corresponds to where the mantle resisting contribution should start to play an important role (Fig. 1A), also favouring lithospheric deformation, as is expected to happen in natural cases (Morra et al., 2006; Schellart et al., 2007).

Hence, we extracted from our modelling database only the models falling into this limited field. Since the η_l/η_{um} ratio affects the way the subduction velocity is partitioned between plate and trench motion, data from models with a constant viscosity contrast have been plotted in V_t vs. V_p space (Fig. 5a–d). Our results confirm the existence of a roughly linear relationship between V_t and V_p (Faccenna et al., 2007), for each η_l/η_{um} ratio by calculating the slope of the regression curves of

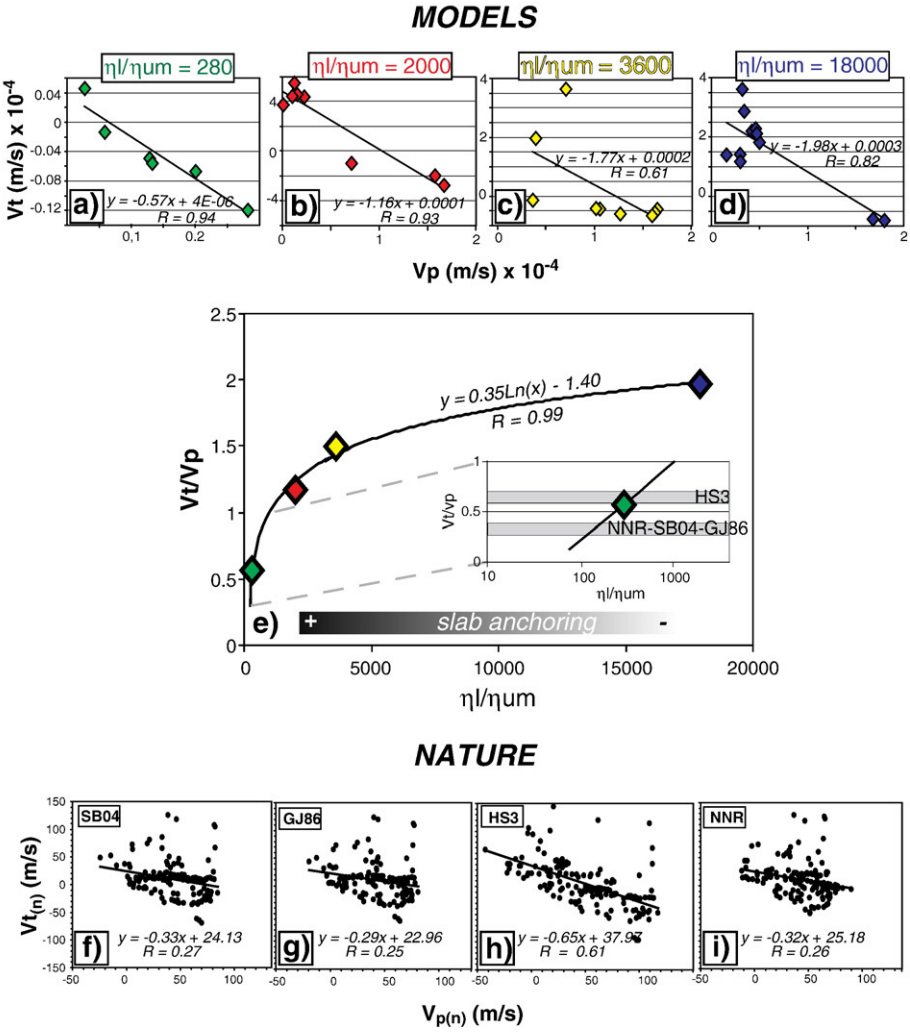

Fig. 5. Velocity field of the normal-to-trench component of the subducting plate and trenches velocity in laboratory models. a) Models characterized by η_l/η_{um}=280; b) models characterized by η_l/η_{um}=2000; c) models characterized by η_l/η_{um}=3600; d) models characterized by η_l/η_{um}=18,000. e) Summarizing diagram showing η_l/η_{um} vs. *Vt/Vp* in models. The colour of points refers to the one adopted in panels a–d. The inset highlights the field interested by natural cases plotted in different absolute reference frames. Velocity field of the normal-to-trench component of the subducting plate and trenches velocity in current subduction zones according to f) SB04; g) GJ86; h) HS3; i) NNR. Regression lines and related correlation coefficients are indicated in each panel.

Fig. 5a–d. Models with η_l/η_{um}=280 are represented by a slope of 0.57 (Fig. 5a; R=0.94), η_l/η_{um}=2000 models have a slope of 1.16 (Fig. 5b; R=0.93), η_l/η_{um}=3600 models have a slope of 1.77 (Fig. 5c; R=0.61), and, models with η_l/η_{um}=18000 gave a slope of 1.98 (Fig. 5d; R=0.82). The slope, therefore, increase with increasing η_l/η_{um}, showing a progressive slow down of plate motion with respect to trench migration. When the experimental data are summarized in the η_l/η_{um} vs. V_t/V_p space (Fig. 5e), it can be seen that V_p contribution controls the subduction process for $\eta_l/\eta_{um}<1000$ while V_t dominates for $\eta_l/\eta_{um}>1000$. In this sense, the diagram also provides insight into the degree of anchoring of the slab within the mantle (Uyeda and Kanamori, 1979). In fact, if V_s is equal to V_p we can assume that the slab does not migrate, being completely anchored to the upper mantle. Alternatively, if V_s is completely absorbed by V_t, then the slab easily moves into the mantle.

The experimental points can be fit by a logarithmic regression (R=0.99; Fig. 5e). The logarithmic decay signifies the progressively decreased role played by the mantle resistance in the subduction system. While a full, quantitative understanding of its origin is still missing (see Supplementary material), this experimental regression represents an important tool to understand experimental subduction models as a function of the viscosity structure and, by inference, to speculate on the natural lithosphere/upper mantle viscosity ratio if kinematic parameters are known.

It is now tempting to examine where Earth parameters are distributed in the diagram shown in Fig. 5e. We have to preliminarily assume that simplified free slab, fluid experiments are meaningful for modelling the Earth's behaviour, and that the V_p–$1/V_t$ relationship holds as a function of η_l/η_{um}, also in current subduction zones. The latter hypothesis is strengthened once the slab is not stationary, but is moving away with respect to the deep anchored slab. This behavior, experimentally insured by the presence of a deep impermeable barrier, seems to occur also in the Earth. Global mantle tomographic images show that slabs tend to be flattened in the transition region (van der Hilst et al., 1991; Fukao et al., 2001), implying that the lithospheric material is transiently ponded on the 660 km phase transition with reduced slab sinking speeds in the lower mantle because of its higher viscosity (Griffiths et al., 1995; Guillou-Frottier et al., 1995; Zhong and Gurnis, 1995a).

For our purposes, kinematic data from current subduction zones in different absolute reference frames are plotted in a $V_{t(n)}$ vs. $V_{p(n)}$ space (Fig. 5f–i), where $V_{t(n)}$ and $V_{p(n)}$ represent the normal components of trench motion and plate motion, respectively. Linear relationships between $V_{t(n)}$ and $V_{p(n)}$ are also observed in natural data, with larger scatter than experimental ones. As expected, the best correlation characterizes the data plot in the HS3 reference frame, as the one in which kinematic data show the widest variability (Fig. 4, Table 2). Mismatches are mainly observed for subduction zones characterized by strong obliquity, narrow trenches, or whose kinematics are strongly forced by mantle flow. Regression coefficients considerably increased by omitting these data, while the slope of the regression curves varies by less than 20%. Natural data show $V_{t(n)}/V_{p(n)}$ values <1 in all selected reference frames, highlighting that from a kinematic point of view $V_{p(n)}$, dominates the velocities involved in the global subduction process. In particular, $V_{p(n)}$ ranges between 0.3 and 0.6 $V_{t(n)}$.

Matching natural to the experimental data shown in Fig. 5e, we observe that a lithosphere/upper mantle viscosity contrast of 150–500 is necessary to obtain realistic trench/subducting plate velocity ratios, as well as the variability of subduction styles recognized in nature. The absolute value of the slab/mantle coupling should be considered only as a first order estimate as the geometry of the curve shown in Fig. 5e is expected to be sensitive to poorly constrained constants. However, the proposed value range is in agreement with other studies (e.g. Mitrovica and Peltier, 1991; King, 1995; Mitrovica and Forte, 1997; Becker et al., 1999; Conrad and Hager, 1999; Billen and Gurnis, 2005).

The relationship between kinematic data and viscous parameters thus emphasizes the importance of the anchoring resistance force (Uyeda and Kanamori, 1979) as previously shown also by our kinematically imposed laboratory models (Heuret et al., 2007). Moreover, our data highlight that the slab directly pulls the incoming plate giving a reasonable connection between trench and plate motions. Furthermore, our results show that systematic, kinematic velocity variations may be linked to slab/mantle viscosity variations. HS3, the reference model characterized by the maximum net rotation (3 times faster than others), requires a viscosity contrast 3 times higher than other, more conservative, net rotation models. In shallow hot spot reference frames, slab/mantle viscosity can increases up to 10^8 (Doglioni et al., 2007).

5. Conclusions

The dynamics of the subduction process has been tested with simplified 3-D tank models under a wide range of parameters and boundary conditions. In particular, the lithosphere/upper mantle viscosity contrast has been varied by four orders of magnitude (~10–10^5), allowing to explore the parameter space between weak and strong slab dynamics.

Our results identify two styles of subduction, distinguished by the partitioning of the subduction velocity between trench and plate velocity: 1) the “retreating mode”, where the slab is shallow dipping and rolls oceanward while the subducting plate slowly moves and 2) the “advancing mode”, where the slab is steep and advances trenchward with a high subducting plate velocity rate. In particular, the retreating mode of subduction is enhanced for $\eta_l/\eta_{um}>10^4$, subduction can occur either with the retreating mode or the advancing mode if η_l/η_{um} ranges between ~10^2 and 10^4, and finally, a Rayleigh–Taylor instability develops for $\eta_l/\eta_{um}<10^2$ (Fig. 2).

Limitations caused by the inherent simplicity of the experimental setting aside, our results can be compared with kinematic data from current subduction zones in four reference frames – hot spot reference frame and no net rotation (NNR) – differing by the amount of net rotation (Figs. 3, 4, Table 2). In all reference frames both trench retreat and trench advance has been observed. Assuming the rate and the style of trench migration is caused by the resistance of mantle to the lateral slab migration and the lithosphere/upper mantle viscosity ratio, plate and trench velocities can be predicted for both models and subduction zones in nature (Fig. 5). Both data-sets show that the plate velocity linearly scales with the trench velocity. Experimental data, furthermore, shows a correlation between V_p/V_t and η_l/η_{um}.

Our results indicate that a lithosphere/upper mantle viscosity contrast of 150–500 is necessary to obtain realistic trench/subducting plate velocity ratios as well as the variability of subduction styles recognized in nature. Furthermore, our results show that velocity differences occurring when plate kinematics is described in different absolute reference frames likely reflect slab/mantle viscosity variations.

Acknowledgements

We thank N. Bellahsen and B. Guillaume for assistance in part of the experimental activity. Discussions with D. Giardini, J. van Hunen, C. Doglioni, G. Morra, N. Ribe and C. Piromallo have been greatly appreciated. We are grateful for the review by an anonymous referee and Claude Jaupart. This research was supported by the CNRS-INSU DyETI program “Dynamics of Subduction”(resp. S.L.) and, as part of the Eurohorcs/ESF — European Young Investigators Awards Scheme (resp. F.F.), by funds from the National Research Council of Italy and other National Funding Agencies participating in the 3rd Memorandum of Understanding, as well as from the EC Sixth Framework Programme. Models have been performed in the “Laboratory of Experimental Tectonics (LET)” Dip. Scienze Geologiche Univ. Roma Tre,

Roma, Italy. We are grateful to *Syral srl* for kindly providing us the glucose syrup used in our models.

Appendix A. Supplementary data

Supplementary data associated with this article can be found, in the online version, at doi:10.1016/j.epsl.2008.04.006.

References

Afonso, J.C., Ranalli, G., Fernandez, M., 2007. Density structure and buoyancy of the oceanic lithosphere revisited. Geophys. Res. Lett. 34 (10).

Ashby, M.F., Verall, R.A., 1978. Micromechanisms of flow and fracture, and their relevance to the rheology of the upper mantle. Philos. Trans. R. Soc. Lond. 288, 59–95.

Becker, T.W., Faccenna, C., O'Connell, R.J., Giardini, D., 1999. The development of slabs in the upper mantle: insights from numerical and laboratory experiments. J. Geophys. Res.-Solid Earth 104 (B7), 15207–15226.

Bellahsen, N., Faccenna, C., Funiciello, F., 2005. Dynamics of subduction and plate motion in laboratory experiments: insights into the "plate tectonics" behavior of the Earth. J. Geophys. Res. 110 (B01401). doi:10.1029/2004JB002999.

Bercovici, D., 1996. Plate generation in a simple model of lithosphere-mantle flow with dynamic self-lubrication. Earth Planet. Sci. Lett. 144, 41–51.

Billen, M.I., Gurnis, M., 2005. Constraints on subducting plate strength within the Kermadec trench. J. Geophys. Res.-Solid Earth 110 (B5).

Buttles, J., Olson, P., 1998. A laboratory model of subduction zone anisotropy. Earth Planet. Sci. Lett. 164 (1–2), 245–262.

Carlson, R.L., Melia, P.J., 1984. Subduction hinge migration. Tectonophysics 102, 1–16.

Cloos, M., 1993. Lithospheric buoyancy and collisional orogenesis — subduction of oceanic plateaus, continental margins, island arcs, spreading ridges, and seamounts. Geol. Soc. Amer. Bull. 105 (6), 715–737.

Conrad, C.P., Hager, B.H., 1999. Effects of plate bending and fault strength at subduction zones on plate dynamics. J. Geophys. Res. 104, 17551–17571.

Crespi, M., Cuffaro, M., Doglioni, C., Giannone, F., Riguzzi, F., 2007. Space geodesy validation of global lithospheric flow. Geophys. J. Int. 168, 491–506.

Davies, G.F., 1995. Penetration of plates and plumes through the mantle transition zone. Earth Planet. Sci. Lett. 133, 507–516.

Doglioni, C., 2008. Comment on "The potential influence of subuction zone polarity on overriding plate deformation, trench migration and slab dip angle" by W.P. Schellart. Tectonophysics. doi:10.1016/j.tecto.2008.02.012.

Doglioni, C., Carminati, E., Cuffaro, M., 2006. Simple kinematics of subduction zones. Int. Geol. Rev. 48 (6), 479–493.

Doglioni, C., Carminati, E., Cuffaro, M., Scrocca, D., 2007. Subduction kinemtics and dynamic constraints. Earth Sci. Rev. 83, 125–175. doi:10.1016/j.earscirev.2007.04.001.

Faccenna, C., Giardini, D., Davy, P., Argentieri, A., 1999. Initiation of subduction at Atlantic-type margins: Insights from laboratory experiments. J. Geophys. Res. 104 (B2), 2749–2766.

Faccenna, C., Heuret, A., Funiciello, F., Lallemand, S., Becker, T.W., 2007. Predicting trench and plate motion from the dynamics of a strong slab. Earth Planet. Sci. Lett. 257 (1–2), 29–36.

Fukao, Y., Widiyantoro, S., Obayashi, M., 2001. Stagnant slabs in the upper and lower mantle transition region. Rev. Geophys. 39 (3), 291–323.

Funiciello, F., Faccenna, C., Giardini, D., Regenauer-Lieb, K., 2003. Dynamics of retreating slabs (part 2): insights from 3D laboratory experiments. J. Geophys. Res. 108 (B4).

Funiciello, F., Faccenna, C., Giardini, D., 2004. Role of lateral mantle flow in the evolution of subduction system: insights from 3-D laboratory experiments. Geophys. J. Int. 157, 1393–1406.

Funiciello, F., Moroni, M., Piromallo, C., Faccenna, C., Cenedese, A., Bui, H.A., 2006. Mapping the flow during retreating subduction: laboratory models analyzed by feature tracking. J. Geophys. Res. 111, B03402 03410.01029/02005JB003792.

Garfunkel, Z., Anderson, D.L., Schubert, G., 1986. Mantle circulation and lateral migration of subducting slabs. J. Geophys. Res. 91, 7205–7223.

Gordon, R.G., Jurdy, D.M., 1986. Cenozoic global plate motions. J. Geophys. Res. 91, 12389–12406.

Griffiths, R.W., Hackney, R.I., Vanderhilst, R.D., 1995. A laboratory investigation of effects of trench migration on the descent of subducted slabs. Earth Planet. Sci. Lett. 133 (1-2), 1–17.

Gripp, A.E., Gordon, R.G., 2002. Young tracks of hot spot and current plate velocities. Geophys. J. Int. 150, 321–361.

Guillou-Frottier, L., Buttles, J., Olson, P., 1995. Laboratory experiments on structure of subducted lithosphere. Earth Planet. Sci. Lett. 133, 19–34.

Heuret, A., 2005. Dynamique des zones de subduction: Etude statistique globale et approche analogique, PhD, Universite' Montpellier II.

Heuret, A., Lallemand, S., 2005. Plate motions, slab dynamics and back-arc deformation. Phys. Earth Planet. Inter. 149 (1–2), 31–51.

Heuret, A., Funiciello, F., Faccenna, C., Lallemand, S., 2007. Plate kinematics, slab shape and back-arc stress: a comparison between laboratory models and current subduction zones. Earth Planet. Sci. Lett. doi:10.1016/j.epsl.2007.02.004.

Jarrard, R.D., 1986. Relations among subduction parameters. Rev. Geophys. 24 (2), 217–284.

Karato, S., 1997. Phase transformation and rheological properties of mantle mineral. In: Crossley, D., Soward, A.M. (Eds.), Phase transformation and rheological properties of mantle mineral. Gordon and Breach, New York, pp. 223–272.

Kincaid, C., Griffiths, R.W., 2003. Laboratory models of the thermal evolution of the mantle during rollback subduction. Nature 425, 58–62.

Kincaid, C., Olson, P., 1987. An experimental study of subduction and slab migration. J. Geophys. Res. 92, 13832–13840.

King, S.D., 1995. Models of mantle viscosity(eds), Models of mantle viscosity, AGU, pp. 227-236.

King, S.D., Masters, G., 1992. An inversion for radial viscosity structure using seismic tomography. Geophys. Res. Lett. 19, 1551–1554.

Kohlstedt, D.L., Evans, B., Mackwell, S.J., 1995. Strength of the lithosphere: constraints imposed by laboratory measurements. J. Geophys. Res. 100 (B9), 17587–17602.

Lallemand, S., 1995. High rates of arc consumption by subduction processes; some consequences. Geology 23, 551–554.

Lallemand, S., Heuret, A., Boutelier, D., 2005. On the relationships between slab dip, back-arc stress, upper plate absolute motion and crustal nature in subduction zones. Geochem. Geophys. Geosyst. 6 (1). doi:10.1029/2005GC000917.

Lithgow-Bertelloni, C., Richards, M.A., 1998. The dynamics of Cenozoic and Mesozoic plate motions. Rev. Geophys. 36, 27–78.

Mitrovica, J.X., Forte, A.M., 1997. Radial profile of mantle viscosity: results from the joint inversion of convection and postglacial rebound observables. J. Geophys. Res.-Solid Earth 102 (B2), 2751–2769.

Mitrovica, J.X., Peltier, W.R., 1991. A complete formalism for the inversion of post-glacial rebound data — resolving power analysis. Geophys. J. Int. 104, 267–288.

Moresi, L., Solomatov, V., 1998. Mantle convection with a brittle lithosphere: thoughts on the global tectonic styles of the Earth and Venus. Geophys. J. Int. 133 (3), 669–682.

Morgan, W.J., 1971. Convection plumes in the lower mantle. Nature 230, 42–43.

Morgan, W.J., 1982. Hotspot tracks and early rifting of the Atlantic. Tectonophysics 94, 123–139.

Morra, G., Regenauer-Lieb, K., Giardini, D., 2006. Curvature of oceanic arcs. Geology 34 (10), 877–880.

O'Neill, C., Muller, D., Steinberger, B., 2005. On the uncertainties in hot spot reconstructions and the significance of moving hot spot reference frames. Geochem. Geophys. Geosyst. 6.

Piromallo, C., Becker, T.W., Funiciello, F., Faccenna, C., 2006. Three-dimensional instantaneous mantle flow induced by subduction. Geophys. Res. Lett. 33 (8) L0830410.0831029/0832005GL0025390.

Ratcliff, J.T., Tackley, P.J., Schubert, G., Zebib, A., 1997. Transitions in thermal convection with strongly variable viscosity. Phys. Earth Planet. Inter. 102 (3-4), 201–212.

Raymond, C.A., Stock, J.M., Cande, S.C., 2000. Fast Paleogene motion of the Pacific hotspots from revised global plate circuit constraints. In: Richards, M.A., Gordon, R.G., Van der Hilst, R.D. (Eds.), Fast Paleogene motion of the Pacific hotspots from revised global plate circuit constraints. Geophysical Monograph, vol. 121. AGU, pp. 359–375.

Ricard, Y., Vigny, C., Froidevaux, J., 1989. Mantle heterogeneities, geoid and plate motion: a MonteCarlo inversion. J. Geophys. Res. 94, 13739–13754.

Sabadini, R., Peltier, W.R., 1981. Pleistocene deglaciation and the Earths rotation: Implications for mantle viscosity. Geophys. J. R. Astron. Soc. 66, 553–578.

Schellart, W.P., 2004. Kinematics of subduction and subduction-induced flow in the upper mantle. J. Geophys. Res. 109 (B7), B07401.

Schellart, W.P., Freeman, J., Stegman, D.R., Moresi, L., May, D., 2007. Evolution and diversity of subduction zones controlled by slab width. Nature 446 (7133), 308–311.

Sdrolias, M., Muller, R.D., 2006. Controls on back-arc basin formation. Geochem. Geophys. Geosyst. 7.

Solomatov, V.S., Moresi, L.-N., 1997. Three regimes of mantle convection with non-Newtonian viscosity and stagnant lid convection in terrestrial planets. Geophys. Res. Lett. 24, 1907–1910.

Spence, W., 1977. Aleutian Arc — Tectonic blocks, episodic subduction, strain diffusion, and magma generation. J. Geophys. Res. 82 (2), 213–230.

Steinberger, B., 2000. Plumes in a convecting mantle: models and observations for individual hotspots. J. Geophys. Res.-Solid Earth 105 (B5), 11127–11152.

Steinberger, B., Sutherland, R., O'Connell, R.J., 2004. Prediction of Hawaiian-Emperor seamount locations from a revised model of global plate motion and mantle flow. Nature 430 (1–2), 167–173.

Tackley, P., 1998. Self-consistent generation of tectonic plates in three-dimensional mantle convection. Earth Planet. Sci. Lett. 157, 9–22.

Trompert, R., Hansen, U., 1998. Mantle convection simulations with rheologies that generate plate-like behaviour. Nature 395, 686–689.

Uyeda, S., Kanamori, H., 1979. Back-arc opening and the mode of subduction. J. Geophys. Res. 84, 1049–1061.

van der Hilst, R., Engdahl, R., Spakman, W., Nolet, G., 1991. Tomographic imaging of subducted lithosphere below northwest Pacific island arcs. Nature 353, 37–43.

Weijermars, R., Schmeling, H., 1986. Scaling of newtonian and non newtonian fluid dynamics without inertia for quantitative modelling of rock flow due to gravity (including the concept of rheological similarity). Phys. Earth Planet. Inter. 43, 316–330.

Zhong, S., Gurnis, M., 1995a. Mantle convection with plates and mobile, faulted plate margins. Science 267, 838–843.

Zhong, S., Gurnis, M., 1995b. Towards a realistic simulation of plate margins in mantle convection. Geophys. Res. Lett. 22, 981–984.